

UDK 621.315.612; 622.785

## Effect of Ga<sub>2</sub>O<sub>3</sub> Addition on the Properties of Y<sub>2</sub>O<sub>3</sub>-Doped AlN Ceramics

H. Shin<sup>\*)</sup>, S.-Ok Yoon, S. Kim, S. Bang

Department of Advanced Ceramic Materials Engineering, Gangneung-Wonju National University, Gangneung, Gangwon-do 210-702, Republic of Korea

---

### Abstract:

*Effect Ga<sub>2</sub>O<sub>3</sub> addition on the densification and properties of Y<sub>2</sub>O<sub>3</sub>-doped AlN ceramics was investigated under the constraint of total sintering additives (Y<sub>2</sub>O<sub>3</sub> and Ga<sub>2</sub>O<sub>3</sub>) of 4.5 wt%. Ga was detected in the AlN grain as well as the grain boundary phases. YAlO<sub>3</sub> and Y<sub>4</sub>Al<sub>2</sub>O<sub>9</sub> were observed as the secondary crystalline phases in all of the investigated compositions. As the substitution of Ga<sub>2</sub>O<sub>3</sub> for Y<sub>2</sub>O<sub>3</sub> increased, the quantity of the Y<sub>4</sub>Al<sub>2</sub>O<sub>9</sub> phase decreased while that of YAlO<sub>3</sub> was more or less similar. Neither additional secondary phases was identified, nor was the sinterability inhibited by the Ga<sub>2</sub>O<sub>3</sub> addition; the linear shrinkage and apparent density were above 20 percent and 3.34-3.37 g/cm<sup>3</sup>, respectively. However, the optical reflectance and the elastic modulus generally decreased whereas the Poisson ratio increased significantly. The dielectric constant and the loss tangent of 4.0Y<sub>2</sub>O<sub>3</sub>-0.5Ga<sub>2</sub>O<sub>3</sub>-95.5Y<sub>2</sub>O<sub>3</sub> at the resonant frequency of 8.22 GHz were 8.63 and 0.003, respectively.*

**Keywords:** Aluminum nitride, Ga<sub>2</sub>O<sub>3</sub>, Optical reflectance, Elastic properties, Dielectric properties.

---

## 1. Introduction

Aluminum nitride (AlN) has received much attention recently in relation to its applications in substrates and packaging materials for high-powered devices, due to its excellent properties such as high thermal conductivity, high electrical resistivity, high dielectric strength, and appropriate thermal expansion coefficient similar to that of silicon [1-3]. It can also be used as a crucible material for molten metals at high temperatures. Furthermore, it is translucent to infrared and visible wavelengths, and it can thus be used as a window material for infrared and radar devices.

AlN requires a fairly high temperature to achieve full density due to its highly covalent bonding and low material diffusivity during sintering. Thus far, three solutions have been proposed to achieve the successful densification of AlN ceramics: (i) use of hot pressing that gives an external driving force for densification; (ii) use of powders with a high specific surface area that promotes diffusion at the surfaces of grains and along grain boundaries during sintering; and (iii) use of sintering additives that form a eutectic liquid between the aluminum oxide in the AlN powder and the additives, which allows densification via liquid-phase sintering [1-3]. As for the route of using sintering additives for the densification of AlN, extensive investigations have been carried out by using various types of additives. Rare earth oxides such as yttria (Y<sub>2</sub>O<sub>3</sub>) and alkaline earth oxides such as calcia (CaO) and

---

<sup>\*)</sup> Corresponding author: hshin@gwnu.ac.kr

magnesia (MgO) have been effective as general sintering additives for high thermal conductivity [3], while fluorides and lithium compounds have proved useful for lowering the sintering temperature;  $\text{Ca}_3\text{Al}_2\text{O}_6$  for improving the translucency; and transition metal oxides for enhancing the shaded colors.

From the viewpoint of sintering mechanism and physical origin that governs the thermal conductivity of sintered AlN, an existing study by Moriya et al. [4] is of particular interest here. These researchers sintered AlN by using a eutectic composition (which forms liquid at 1760°C) in the  $\text{Y}_2\text{O}_3$ - $\text{Al}_2\text{O}_3$  system and reported that a sudden change of the grain size and shape occurred at 1750°C, while the formation of the neck between the AlN particles progressed in the temperature range of 1600–1700°C. Based on the observation of very low thermal conductivity values of their samples, it was suggested that the high oxygen concentration in the AlN lattice needs to be eliminated by the action of the sintering additives to ensure a high thermal conductivity.

To our knowledge, no study has been carried out to investigate the effect of substituting  $\text{Ga}_2\text{O}_3$  for the  $\text{Y}_2\text{O}_3$  sintering additive on the resultant properties of sintered AlN ceramics. The present study systematically investigates the effect of the substitution of  $\text{Ga}_2\text{O}_3$  for  $\text{Y}_2\text{O}_3$  under the constraint of total sintering additives ( $\text{Y}_2\text{O}_3$  and  $\text{Ga}_2\text{O}_3$ ) of 4.5 wt%, and reports the densification, crystal phase evolution, optical reflectance, and elastic and dielectric properties of the sintered specimens.

## 2. Experimental procedure

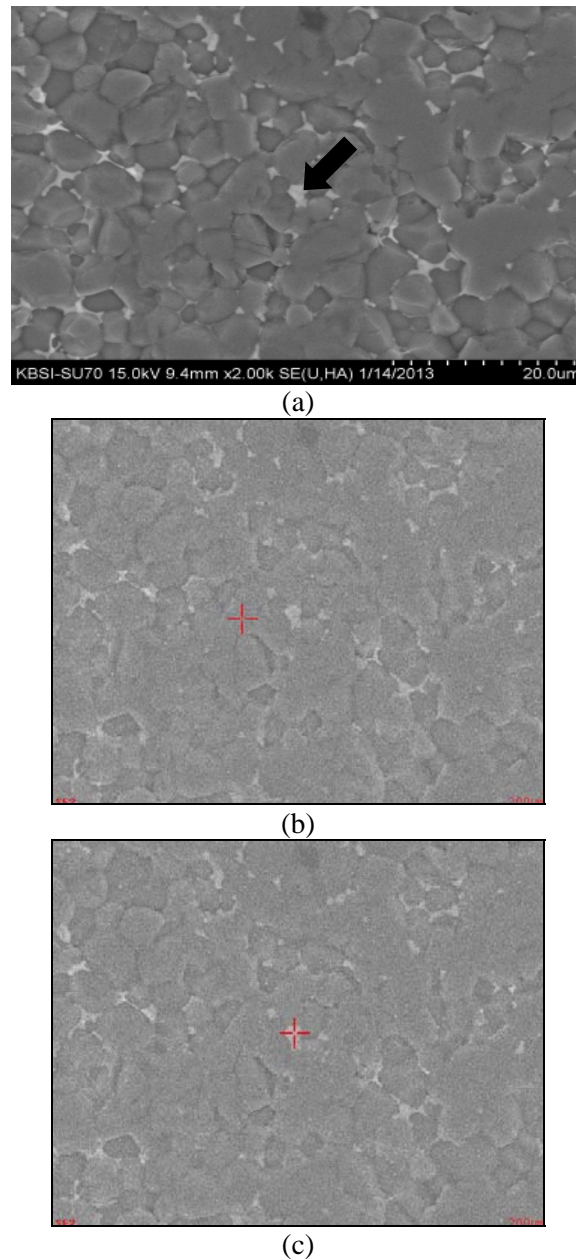
AlN (H grade, Tokuyama Co. Ltd., Japan, 0.85 wt% oxygen),  $\text{Y}_2\text{O}_3$  (Purity 4N, High Purity Chemicals Co. Ltd, Japan), and  $\text{Ga}_2\text{O}_3$  (Purity 3N, High Purity Chemicals Co. Ltd, Japan) were used as starting powders. The total amount of sintering additives was 4.5 wt% and the prepared compositions were  $(4.5-x)\text{Y}_2\text{O}_3 - x\text{Ga}_2\text{O}_3 - 95.5\text{AlN}$ , where  $x = 0, 0.25, 0.50, 0.75$ , and 1.00. A 20g batch was ball milled by  $\text{ZrO}_2$  balls under ethanol medium in a polyethylene-based container for 5h followed, respectively, by periods of drying in an oven, uniaxial pressing at 100 MPa to form a disk shape, and cold isostatic pressing at 200 MPa. The disk-shaped specimens were shifted to a BN-coated graphite crucible, heat treated at 400°C for 2h, and sintered at 1800°C for 3h in a graphite furnace. The heat treatment and sintering were carried out in a flowing  $\text{N}_2$  atmosphere (1 L/min) at 1 atm.

The apparent density of the sintered specimens was measured by the Archimedes principle using an ethanol medium. The crystalline phases of the sintered specimen were identified by a powder X-ray diffractometer (Model X'pert PRO MPD, PANalytical, Ea Almelo, the Netherlands) using pulverized powder. The microstructure of the sintered specimen was characterized by a field emission scanning electron microscope (FESEM, Model SU-70, Hitachi, Tokyo, Japan)<sup>1</sup>. A compositional analysis of the grain and grain boundary was performed by an energy dispersive spectroscopy (EDS, Model Pegasus XM4, EDAX Inc., Mahwah, NJ, USA). The optical reflectance of the sintered specimens was measured after mirror polishing of the surface by a spectrophotometer in the wavelength range from 200 to 800nm (Model V650, JASCO International Co., Ltd., Tokyo, Japan). The elastic modulus and Poisson ratio were determined by the ultrasonic pulse-echo technique (Model UT340, UTEX Scientific Instruments Inc., Mississauga, Ontario, Canada). The microwave dielectric properties of the sintered disk specimens were measured by using a network analyzer (E5071C ENA, 100 kHz–8.5 GHz; Agilent Technologies, Palo Alto, CA, USA) with the Hakki–Coleman fixture configuration [5].

<sup>1</sup>Korea Basic Science Institute (KBSI) at Gangneung, Gangwon-do, Republic of Korea

### 3. Results and Discussion

The microstructure of  $\text{Y}_2\text{O}_3$  and  $\text{Ga}_2\text{O}_3$ -doped  $\text{AlN}$  ceramics observed by the secondary electron (SE) mode of FE-SEM, and the typical microstructure, are shown in Fig. 1 for the case when  $x = 0.50$  in  $(4.5-x)\text{Y}_2\text{O}_3 - x\text{Ga}_2\text{O}_3 - 95.5\text{AlN}$  system. The arrow marked in Fig. 1(a) indicates the secondary phase with a brighter color than in the  $\text{AlN}$  matrix. When the coating thickness on the specimen surface is thin enough, a chemical contrast can be observed in the SE mode, which is the case for the secondary phase herein (marked by the arrow). The brighter color indicates that the secondary phase is composed of a heavier element than the  $\text{AlN}$  grain, such as Y and Ga.

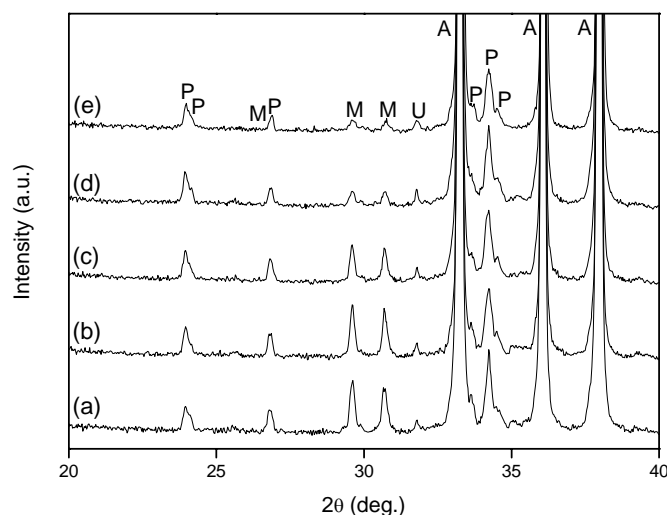


**Fig. 1.** (a) FESEM micrograph for the sintered  $\text{AlN}$  with  $x=0.5$ , (b) EDS spot position on the grain, and (c) EDS spot position on the grain boundary.

**Tab. I** Chemical composition of grain and grain boundary for x=0.50 sample analyzed by EDS (wt%).

Element	Grain	Grain boundary
Al	81.85	29.69
Y	-	48.84
Ga	0.63	0.57
N	17.52	9.64
O	-	11.27

The crosses marked in Figs 2(b) and 2(c) indicate the spot positions for the EDS analysis in the grain and on the grain boundary, respectively. The resultant chemical compositions determined by the EDS analysis are shown in Tab. I. As seen in the table, the grain boundary is rich in Al, Y, Ga, O and N, whereas Al, Ga, and N are rich in the grain. It is interesting to note that Ga is detected in the AlN grain as well as on the grain boundary. The dissolution of  $\text{Al}_2\text{O}_3$  into the AlN lattice during the sintering process is well documented [6]. Yet, to our knowledge, there has been no study conducted on the existence of Ga in the AlN structure; the similar ionic size between Al and Ga might result in the partial dissolution of Ga into the AlN lattice, although not to a significant degree (i.e. the concentration of Ga is small compared to that of Al in the grain). This point will be discussed further at a later point in this paper, together with a discussion of the composition of the grain boundary phases.

**Fig. 2.** Powder XRD patterns of  $\text{Y}_2\text{O}_3$  and  $\text{Ga}_2\text{O}_3$ -doped AlN ceramics at 1800°C for 3h; (a) x=0, (b) 0.25, (c) 0.50, (d) 0.75, and (e) 1.0 (A: AlN, P:  $\text{YAlO}_3$ , M:  $\text{Y}_4\text{Al}_2\text{O}_9$ , and U: unidentified phase).

The powder X-ray diffraction patterns of the sintered specimens are shown in Fig. 2. When no  $\text{Ga}_2\text{O}_3$  is added (x=0), AlN is identified as the main phase, and  $\text{YAlO}_3$  with an orthorhombic perovskite structure and  $\text{Y}_4\text{Al}_2\text{O}_9$  with a monoclinic structure are observed as the secondary phases. There are three compounds of  $\text{Y}_3\text{Al}_5\text{O}_{12}$ ,  $\text{YAlO}_3$ , and  $\text{Y}_4\text{Al}_2\text{O}_9$  in the  $\text{Y}_2\text{O}_3$ - $\text{Al}_2\text{O}_3$  system. Ueno [2] reported the types of grain boundary phases in AlN ceramics sintered at 1800°C for 2h with a varying amount of  $\text{Y}_2\text{O}_3$ , where the oxygen content of the starting AlN powder was assumed to be 1 wt%. In Ueno's study,  $\text{YAlO}_3$  formed in the composition range of 1.5-6 wt%  $\text{Y}_2\text{O}_3$ , while  $\text{Y}_4\text{Al}_2\text{O}_9$  formed additionally in the 3-6 wt% range of  $\text{Y}_2\text{O}_3$ . His result is consistent with that of the current study in that  $\text{YAlO}_3$  and  $\text{Y}_4\text{Al}_2\text{O}_9$  are observed in the investigated composition range of 3.0-4.5 wt%  $\text{Y}_2\text{O}_3$ .

As the degree of substitution of  $\text{Ga}_2\text{O}_3$  for  $\text{Y}_2\text{O}_3$  increased, the quantity of  $\text{Y}_4\text{Al}_2\text{O}_9$  phase decreased while that of  $\text{YAlO}_3$  was more or less similar based on the comparison of the peak intensities. For the  $\text{Ga}_2\text{O}_3$ -substituted specimens, no additional phases such as gallium oxynitride or yttrium gallate ( $\text{Y}_3\text{GaO}_6$ ) were identified, as shown in Fig. 2. It was reported that aluminum oxynitride ( $\text{Al}_3\text{O}_3\text{N}$ ) formed in the  $\text{Al}_2\text{O}_3$  and  $\text{Y}_2\text{O}_3$ -doped AlN system sintered above  $1650^\circ\text{C}$  [4]. Popova et al. [7] pointed out that  $\text{Y}_3\text{GaO}_6$ , which is one of the compounds in the  $\text{Y}_2\text{O}_3$ - $\text{Ga}_2\text{O}_3$  system, formed above  $1300^\circ\text{C}$  and was stable up to the melting temperature ( $1850^\circ\text{C}$ ). These results suggest the possibility of Ga substitution for Al in the secondary crystalline phases; a solid solution may form between the yttrium aluminates and yttrium gallates due to the similar ionic size of the Ga-to-Al ion. However, as mentioned, the degree of Ga substitution for Al might not be significant due to the low Ga concentration in the grain compared to the amount of Al. Further, no significant shift of diffracted peaks of  $\text{YAlO}_3$  and  $\text{Y}_4\text{Al}_2\text{O}_9$  was observed.

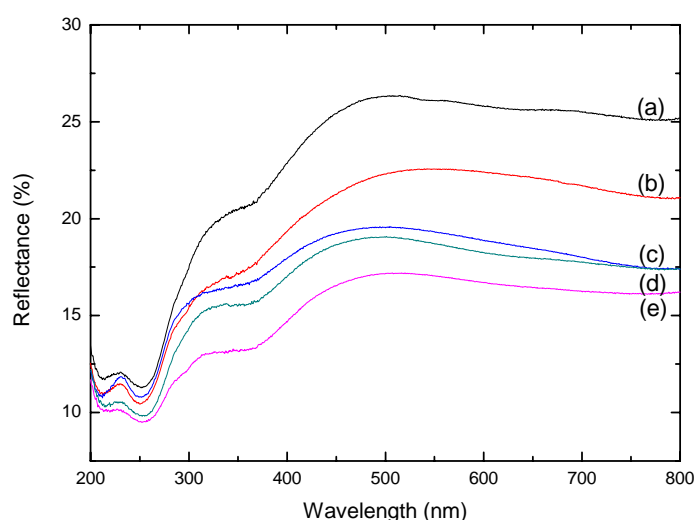


**Fig. 3.** Reflectance spectra of  $\text{Y}_2\text{O}_3$  and  $\text{Ga}_2\text{O}_3$ -doped AlN ceramics at  $1800^\circ\text{C}$  for 3h; (a)  $x=0$ , (b) 0.25, (c) 0.50, (d) 0.75, and (e) 1.0.

The optical reflectance spectra of  $\text{Y}_2\text{O}_3$  and  $\text{Ga}_2\text{O}_3$ -doped AlN ceramics in the ultraviolet and visible-light wavelength ranges are shown in Fig. 3. The reflectance of the specimen with  $x = 0$  in the visible-light wavelength regime (400-700 nm) is approximately 25 percent. The specimen is gray or dark gray in color. As the amount of  $\text{Ga}_2\text{O}_3$  increases, the reflectance of specimens decreases. As shown in Fig. 2, the quantity of  $\text{Y}_4\text{Al}_2\text{O}_9$  phase decreases with  $\text{Ga}_2\text{O}_3$ . This observation suggests that the decreased quantity of  $\text{Y}_4\text{Al}_2\text{O}_9$  phase may be responsible for the decreased optical reflectance, although further study is necessary to fully clarify this issue.

The linear shrinkage, apparent density, elastic and dielectric properties of  $\text{Y}_2\text{O}_3$  and  $\text{Ga}_2\text{O}_3$ -doped AlN ceramics are shown in Tab. II. When no  $\text{Ga}_2\text{O}_3$  is added ( $x=0$ ), the linear shrinkage of the specimen is 20.8 percent after the sintering at  $1800^\circ\text{C}$  for 3h, whereas that of the  $\text{Ga}_2\text{O}_3$ -added specimens is between 20.2 and 21.1 percent, indicating that the substitution of  $\text{Ga}_2\text{O}_3$  for  $\text{Y}_2\text{O}_3$  does not inhibit the sinterability of the AlN ceramics. The apparent density of the sintered specimens in the current study is in the range of  $3.34\text{--}3.37\text{ g/cm}^3$ , which is higher than that of pure AlN ( $3.26\text{ g/cm}^3$ ) due to the formation of the secondary crystalline phases with higher densities;  $5.35$  and  $4.52\text{ g/cm}^3$  for  $\text{AlO}_3$  and  $\text{Y}_4\text{Al}_2\text{O}_9$ , respectively [8-9].

As shown in Tab. II, the elastic modulus generally decreases from 362 ( $x = 0$ ) to 335 GPa ( $x = 1.0$ ) by the addition of  $\text{Ga}_2\text{O}_3$ . These values are higher than those of polycrystalline AlN (308-322 GPa [10-12]) but lower than those of single crystal AlN (374 GPa [13]). Considering that the reported elastic moduli of  $\text{YAlO}_3$  and  $\text{Y}_4\text{Al}_2\text{O}_9$  are 318 [14] and 190 GPa

[14], respectively, our result for  $x = 0$  (362 GPa) is fairly high. Further work is therefore necessary to seek the origin of such a high elastic modulus. The decreasing trend of the elastic modulus with  $x$  is observed despite the decreasing phase quantity of  $Y_4Al_2O_9$ . Thus, it is interpreted that the gallium present in the AlN grain and secondary phases (increase of  $x$ ) generally decreases the elastic modulus.

**Tab. II** The linear shrinkage, bulk density, and properties of  $Y_2O_3$  and  $Ga_2O_3$ -doped AlN ceramics

x	Linear shrinkage (%)	Apparent density ( $g/cm^3$ )	Elastic modulus (GPa)	Poisson's ratio	Dielectric constant	Resonant frequency (GHz)	Loss tangent / $10^{-3}$
0	20.8	3.34	362	0.146	8.63	8.27	2.65
0.25	20.6	3.36	321	0.251	8.59	8.36	2.98
0.50	21.1	3.37	352	0.250	8.63	8.22	3.02
0.75	21.0	3.37	342	0.233	8.55	8.23	2.76
1.0	20.2	3.37	335	0.237	8.82	8.40	3.95

The Poisson ratio of the  $Y_2O_3$ -only-added specimen ( $x = 0$ ) is 0.146, which is slightly lower than that of the polycrystalline AlN (0.179 [10] or 0.245 [11]). The addition of  $Ga_2O_3$  increases the Poisson ratio significantly, which will be influenced by the complicated roles of the secondary phases (decreasing phase quantity of  $Y_4Al_2O_9$  and similar quantity of  $YAlO_3$  with increased  $x$ ) and the phenomenon of Ga doping to the AlN grain and grain boundary.

The dielectric constant and the loss tangent of  $Y_2O_3$ -only-doped AlN are 8.63 and 0.00265, respectively, at a resonance frequency of 8.27 GHz. These dielectric properties are not much changed by the addition of  $Ga_2O_3$  as compared to the mechanical properties. The value of the loss tangent is about ten times larger than that of commercial AlN substrates. Savrun and Nguyen [15] reported that there was a wide range of the loss tangent for AlN ceramics between 0.01 and 0.0005. According to their research, this wide range results from the differences between the processing techniques and the raw materials.

#### 4. Conclusion

Effect  $Ga_2O_3$  addition on the densification, phase evolution, optical reflectance, elastic modulus, and dielectric properties of  $Y_2O_3$ -doped AlN ceramics sintered at 1800°C for 3h was investigated under the constraint of total sintering additives ( $Y_2O_3$  and  $Ga_2O_3$ ) of 4.5 wt%. Based on an EDS analysis, the grain boundary phase was rich in Al, Y, Ga, O, and N, whereas Al, Ga, and N were identified in the grain. The similar ionic size of the Ga-to-Al ion might result in the dissolution of Ga into the AlN lattice, although not to a significant degree, as the concentration of Ga is very small in the grain compared to Al. AlN was identified as the main crystalline phase, whereas  $YAlO_3$  with an orthorhombic perovskite structure and  $Y_4Al_2O_9$  with a monoclinic structure were observed as the secondary phases. As the degree of substitution of  $Ga_2O_3$  for  $Y_2O_3$  increased, the amount of  $Y_4Al_2O_9$  decreased while that of  $YAlO_3$  was more or less similar. Neither additional secondary phases was identified, nor was the sinterability inhibited by the increased  $Ga_2O_3$ ; the linear shrinkage and the apparent density were above 20 percent and 3.34-3.37  $g/cm^3$ , respectively. However, the optical reflectance and the elastic modulus generally decreased, whereas the Poisson ratio increased significantly. The dielectric properties were not much changed by the  $Ga_2O_3$  addition as compared to the mechanical properties. The dielectric constant and the loss tangent of

$4.0\text{Y}_2\text{O}_3\text{-}0.5\text{Ga}_2\text{O}_3\text{-}95.5\text{Y}_2\text{O}_3$  at the resonant frequency of 8.22 GHz were 8.63 and 0.003, respectively.

## Acknowledgments

This study was supported by the Human Resource Training Project for Regional Innovation, funded by the Ministry of Education, Science, and Technology (MEST) through the National Research Foundation (NRF) of Korea. The authors appreciate the technical assistance of Mr. Injoon Hwang.

## 5. References

1. G. V. Samsonov, T. V. Dubovik, T. V. Andreeva, B. V. Sharovskii, V. F. Litvinenko, Sci. Sinter., 12 (1980) 131.
2. F. Ueno, Electric Refractory Materials, Marcel Dekker, Inc., New York, 2000.
3. A. Kranzmann, P. Greil, G. Petzow, Sci. Sinter., 20 (1988) 135.
4. Y. Moriya, M. Imamura, M. Kasori, K. Oishi, J. Ceram. Soc. Jpn., 112 (2004) 280.
5. B. W. Hakki, P. D. Coleman, IRE Trans. Microwave Theory Tech., 8 (1960) 402.
6. M. F. Denanot, J. Rabier, J. Mat. Sci., 24 (1989) 1594.
7. V. F. Popova, A. G. Petrosyan, E. A. Tugova, D. P. Romanov, V. V. Gusarov, Russ. J. Inorg. Chem., 54 (2009) 624.
8. Powder Diffraction File 33-0041, International Center for Diffraction Data (ICDD).
9. Powder Diffraction File 34-0368, International Center for Diffraction Data (ICDD).
10. D. Gerlich, S. L. Dole, G. A. Slack, J. Phys. Chem. Solids, 47 (1986) 437.
11. P. Boch, J. C. Glandus, J. Jarrige, J. P. Lecompte, J. Mexmain, Ceram. Int., 8 (1982) 34.
12. R. Ruh, A. Zangvil and J. Barlowe: Am. Ceram. Soc. Bull., 64 (1985) 1368.
13. I. Yonenaga, T. Shima, M. H. F. Sluiter, Jpn. J. Appl. Phys., 41 (2002) 4620.
14. X. Zhan, Z. Li, B. Liu, J. Wang, Y. Zhou, Z. Hu, J. Am. Ceram. Soc., 95 (2012) 1429.
15. E. Savrun, V. Nguyen, "7th IEEE International Vacuum Electronics Conference," Ed. B. Fickett, Institute of Electrical and Electronics Engineers (IEEE), 2006, p. 35.

**Садржај:** Испитиван је утицај додатка  $\text{Ga}_2\text{O}_3$  на згушњавање и својства керамике  $\text{Y}_2\text{O}_3$ -допираног  $\text{AlN}$  са ограниченом концентрацијом адитива ( $\text{Y}_2\text{O}_3$  и  $\text{Ga}_2\text{O}_3$ ) од 4,5 wt%.  $\text{Ga}$  је детектован у зрнима  $\text{AlN}$  као и на границама фаза.  $\text{YAlO}_3$  и  $\text{Y}_4\text{Al}_2\text{O}_9$  су уочене као секундарне кристалне фазе у свим испитиваним једињењима. Како је суституција  $\text{Ga}_2\text{O}_3$  са  $\text{Y}_2\text{O}_3$  расла, количина  $\text{Y}_4\text{Al}_2\text{O}_9$  фазе је опадала док је  $\text{YAlO}_3$  остао исти. Нису детектоване додатне секундарне фазе, нити је синтероване инхибирано додатком  $\text{Ga}_2\text{O}_3$ ; линеарно скупљање и привидна густина су биле преко 20 процената и  $3,34\text{-}3,37\text{ g/cm}^3$ , истим редоследом. Ипак, вредности рефлексије и модула еластичности генерално опадају док је Поасонов однос значајно порастао. Диелектрична константа и тангенс губитака  $4,0\text{Y}_2\text{O}_3\text{-}0,5\text{Ga}_2\text{O}_3\text{-}95,5\text{Y}_2\text{O}_3$  на резонантној фреквенцији од 8,22 GHz су износили 8,63 и 0,003, истим редоследом.

**Кључне речи:** алуминијум нитрид,  $\text{Ga}_2\text{O}_3$ , рефлексија, еластична својства, диелектрична својства